Current Biology 16, 543–552, March 21, 2006 ©2006 Elsevier Ltd All rights reserved DOI 10.1016/j.cub.2006.01.051

Article

Developmental Control of Nuclear Size and Shape by *kugelkern* and *kurzkern*

Annely Brandt,[1,*] Fani Papagiannouli,[1] Nicole Wagner,[2] Michaela Wilsch-Bräuninger,[3] Martina Braun,[4] Eileen E. Furlong,[4] Silke Loserth,[2] Christian Wenzl,[1] Fanny Pilot,[5] Nina Vogt,[6] Thomas Lecuit,[5] Georg Krohne,[2] and Jörg Großhans[1]

[1] Zentrum für Molekulare Biologie der Universität Heidelberg (ZMBH)
Im Neuenheimer Feld 282
69120 Heidelberg
Germany

[2] Biozentrum
Universität Würzburg
Am Hubland
97074 Würzburg
Germany

[3] Max-Planck-Institut für Molekulare Zellbiologie und Genetik
Pfotenhauerstr. 108
01307 Dresden
Germany

[4] European Molecular Biology Laboratory
Meyerhofstrasse 1
69117 Heidelberg
Germany

[5] Institut de Biologie du Développement de Marseille (IBDM)
Laboratoire de Génétique et de Physiologie du Développement (LGPD)
Centre National de la Recherche Scientifique
Unité Mixte de Recherche 6545
Université de la Méditerrannée
Campus de Luminy, case 907
13288 Marseille Cedex 09
France

[6] Max-Planck-Institut für Entwicklungsbiologie
Spemannstr. 35,
72076 Tübingen
Germany

Summary

Background: The shape of a nucleus depends on the nuclear lamina, which is tightly associated with the inner nuclear membrane and on the interaction with the cytoskeleton. However, the mechanism connecting the differentiation state of a cell to the shape changes of its nucleus are not well understood. We investigated this question in early *Drosophila* embryos, where the nuclear shape changes from spherical to ellipsoidal together with a 2.5-fold increase in nuclear length during cellularization.

Results: We identified two genes, *kugelkern* and *kurzkern*, required for nuclear elongation. In *kugelkern*- and *kurzkern*-depleted embryos, the nuclei reach only half the length of the wild-type nuclei at the end of cellularization. The reduced nuclear size affects chromocenter formation as marked by Heterochromatin protein 1 and expression of a specific set of genes, including early zygotic genes. *kugelkern* contains a putative coiled-coil domain in the N-terminal half of the protein, a nuclear localization signal (NLS), and a C-terminal CxxM-motif. The carboxyterminal CxxM motif is required for the targeting of Kugelkern to the inner nuclear membrane, where it colocalizes with lamins. Depending on the farnesylation motif, expression of *kugelkern* in *Drosophila* embryos or *Xenopus* cells induces overproliferation of nuclear membrane.

Conclusions: Kugelkern is so far the first nuclear protein, except for lamins, that contains a farnesylation site. Our findings suggest that Kugelkern is a rate-determining factor for nuclear size increase. We propose that association of farnesylated Kugelkern with the inner nuclear membrane induces expansion of nuclear surface area, allowing nuclear growth.

Introduction

The morphology of nuclei varies among different developmental stages, tissues, and cell-cycle states. Age-related alterations of nuclear shape, accompanied by loss of peripheral heterochromatin, have been found in *C. elegans* [1] as well as in human cell lines [2]. Abnormalities in nuclear size and shape are frequently observed in malignant tissues [3] or in patients with nuclear envelopathies or certain progeria syndromes [2]. In addition, there is growing evidence that the nuclear lamina has not only structural but also functional impact on the cell by regulating chromatin configuration and influencing gene expression (for review, see [4]). The mechanisms that link the morphology of the nucleus to the developmental program of a cell have not been much analyzed (for review, see [4, 5]).

The shape of a nucleus depends on the nuclear lamina, which is thought to provide mechanical support for the nuclear membrane (NM) and to mediate attachment of interphase chromatin to the nuclear envelope [6, 7]. The lamina consists of a meshwork of nuclear-specific intermediate filaments, the lamin proteins, plus numerous lamin-associated proteins (for review, see [4, 7]). Targeting and association of lamins with the inner membrane is mediated by an evolutionary conserved farnesylation of the CxxM motif at their C termini (for review, see [8, 9]).

In *Drosophila* development, there is a definite event of nuclear shape change, accompanied by massive nuclear growth during the process of cellularization [10]. During cellularization, all cortical nuclei are simultaneously enclosed into membranes, and there is a marked change in the shape of the nuclei from spherical to ellipsoid together with a 2.5-fold increase in nuclear length [11, 12]. The mechanisms and components involved have remained elusive.

*Correspondence: a.haase@zmbh.uni-heidelberg.de

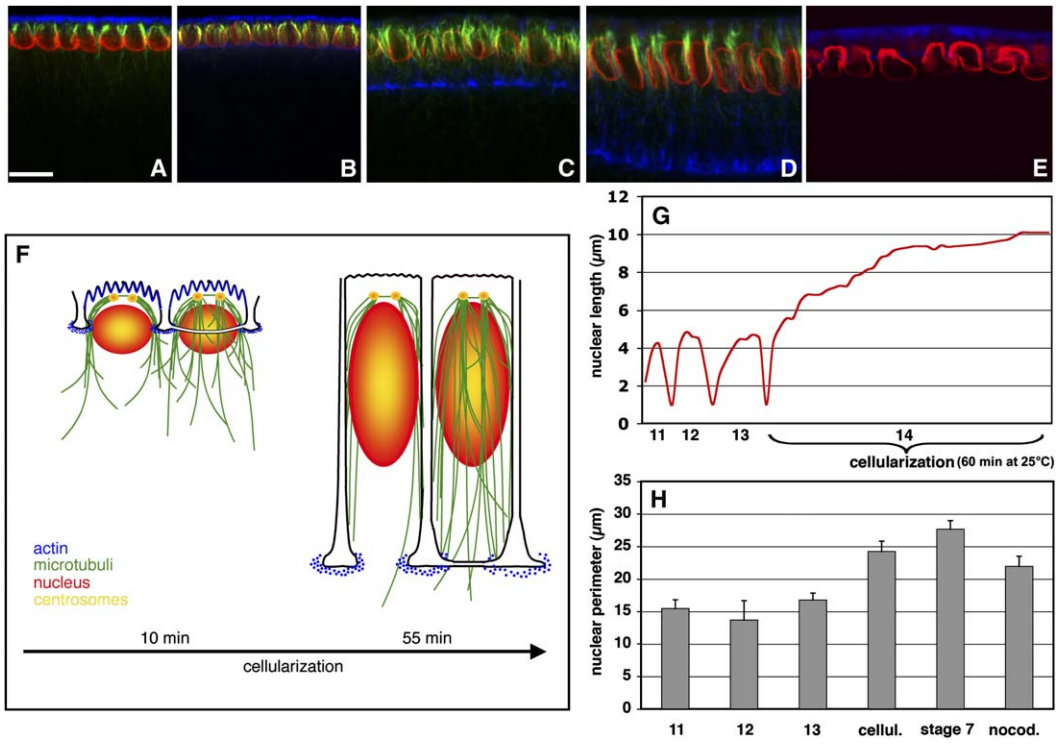

Figure 1. Nuclear Shape Change during Cellularization

(A–E) Wild-type embryos during cellularization stained for Kuk (red), F-actin (blue), and microtubules (green). The scale bar represents 10 μm.
(E) Nocodazole-treated embryo; note the absence of microtubuli (green).
(F) Schematic overview of cellularization.
(G) Kinetics of nuclear length (apical-basal axis) during cell cycles 11 to 14.
(H) Perimeter of interphase nuclei in different cell cycles, in gastrulation (stage 7) or in nocodazole-treated embryos. n = 30 for each group, error bars = standard deviation. For untreated (cellul.) versus nocodazole-treated (nocod.) embryos: n = 30, nondirectional Mann-Whitney test, $p > 0.05$, $U_A = 580$, $z = -1.91$. For cycle-13 embryos versus nocodazole-treated embryos: n = 30, nondirectional Mann-Whitney test, $p < 0.01$, $U_A = 867$, $z = -6.16$.

The early syncytial blastoderm is characterized by rapid nuclear division cycles, transcriptional silencing, and a homogeneous appearance of the chromatin. At the transition from syncytial to cellular blastoderm, the cell cycle is paused, the transcription rate increases, and chromatin loses its uniform appearance. This change in chromatin organization is highlighted by the appearance of a conspicuous chromocenter [13]. Strikingly, this reorganization of the chromatin takes place during cycle 14 and coincides with the strong increase of zygotic transcription and nuclear elongation.

Results

Nuclear Elongation during Cellularization

During cellularization, the shape of the nuclei changes from spherical to ellipsoidal together with a 2.5-fold increase in nuclear length from approximately 4 μm up to 10 μm (Figures 1A–1D, 1F, and 1G). A rearrangement of the microtubuli-based cytoskeleton accompanies membrane invagination and nuclear shape change [11]. As the nucleus assumes an elongated appearance, microtubules extend in close association with the nucleus, mirroring nuclear growth in both direction and rate [11]. To determine whether the nuclear growth depends on microtubules, we treated staged embryos with the microtubule (MT) polymerization inhibitor nocodazole. After incubation in nocodazole, the nuclei maintained a rounded, irregular shape although their nuclear surface area increased significantly in size (Figures 1E and 1H). Confirming data from [14], we found that MT function is essential for the shape change of the nuclei from spherical to ellipsoidal but not for the nuclear growth.

kugelkern and *kurzkern* Are Required for Nuclear Elongation

We identified two genes required for the process of nuclear elongation in independent screens for genes involved in blastoderm formation. *kugelkern* (*kuk*) was identified by its early zygotic expression (see Experimental Procedures). In embryos injected with *kuk* dsRNA (designated *kuk* embryos) or from *kuk*-deficient females (Figures S1A and S1B in the Supplemental Data available online), the cortical nuclei are spherical by the end of cellularization (Figure 2A). The nuclei reached only the same length as in previous interphases (4 μm) as compared to wild-type nuclei that finally reached 10 μm in length (Figure 2B). Nevertheless, the cellularization front invaginated with the same velocity as in wild-type embryos. Microtubules and the actin cytoskeleton seemed to be unaffected (Figure 2A, compare to Figure 1D). We could not find any obvious

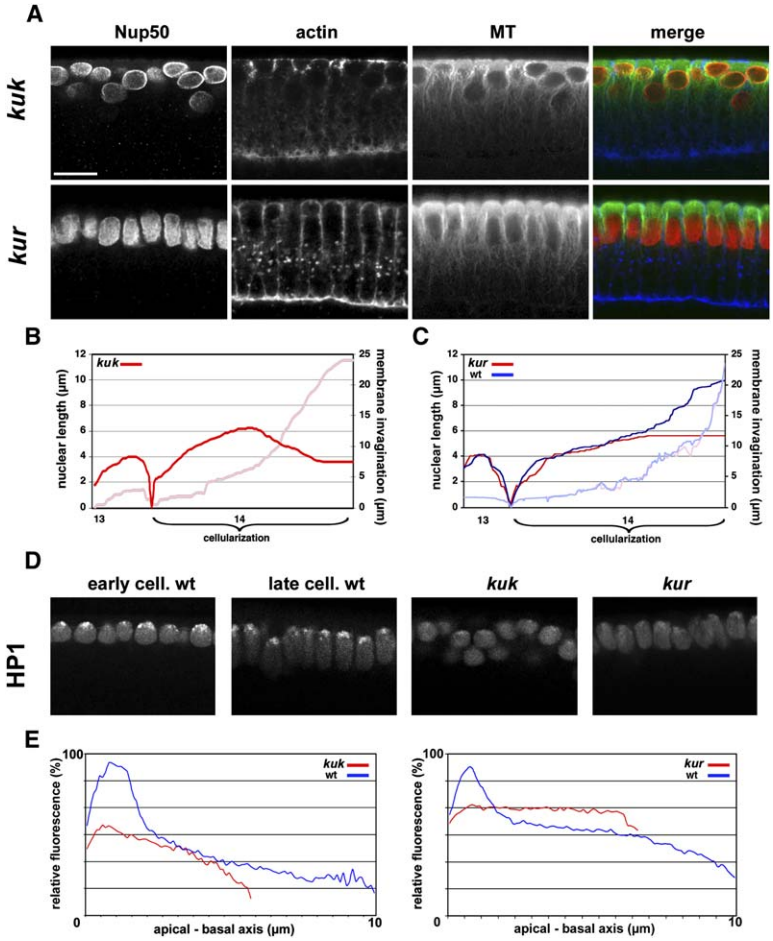

Figure 2. Phenotype of *kuk* and *kur*

(A) *kuk*-RNAi-treated embryo and *kur* embryos at the end of cellularization stained with anti-Nup50 (red), anti-α-Tubulin (green) antibodies, and phalloidin (blue); the scale bar represents 10 μm.

(B and C) Kinetics of nuclear length increase and membrane invagination during interphases of cell cycles 13 and 14. Blue line shows nuclear length of wild-type embryos; red line shows *kuk*-deficient embryos (B) or *kur* embryos (C). Length of invaginated membrane is depicted in light blue (wt) and light red (*kuk*/*kur*).

(D) HP1 staining in wild-type at early and late cellularization or in *kuk* and *kur* embryos late during cellularization.

(E) Relative fluorescence of HP1 staining along the apical-basal axis of the nuclei in wild-type *kuk* (RNAi-treated) and *kur* embryos.

morphological differences between *kuk* and wild-type embryos with regard to the positioning of the nuclei by the end of cellularization (data not shown). *kuk* is not an essential gene, because *kuk*-deficient flies are viable and fertile.

In embryos from *kurzkern* (*kur)* germline clones (*kur* embryos), nuclear elongation was significantly reduced. There was no visible defect prior to cellularization in *kur* embryos when compared to wild-type embryos (Figure 2C). The nuclei of *kur* mutants started to elongate normally in the first half of cellularization. When the invaginating membrane front reached the basal outline of the nuclei, the first retardation compared to the wild-type situation was observed (Figure 2C). Finally, the nuclei accomplished only approximately 60% of the length of wild-type nuclei at the end of cellularization (Figures 2A and 2C). However, in contrast to the wild-type situation, *kur* nuclei did not move basally at the end of cellularization. During gastrulation, *kur* embryos fail to form the cephalic furrow and do not accomplish germband extension; this is comparable to the germband-extension phenotype of *eve* described by [15]. Because this gastrulation phenotype was different from that found in *kuk* embryos, it may represent a second function of *kur* independent of the earlier nuclear-elongation function. In conclusion, we identified two genes, *kuk* and *kur*, that are required for nuclear elongation during cellularization.

kuk and *kur* Affect Chromocenter Formation and Correct Gene Expression

During cellularization, a chromocenter is formed by centromeric heterochromatin, which remains condensed even in interphases [13]. At early stages of development, the chromatin is homogenous in appearance and the heterochromatin marker Heterochromatin protein 1 (HP1) is present throughout the nucleoplasm (Figure 2D). During cellularization, HP1 accumulates at the apical-located chromocenter, whereas reduced amounts of the protein are present basally in the nucleus (Figure 2D, [13]).

In *kuk* or *kur* embryos, the formation of a distinct chromocenter was impaired. In many nuclei, the strong apical HP1 staining was absent (Figure 2D). In only few nuclei, a very weakly stained chromocenter was detectable when compared to the wild-type situation at the same stage of development. Conspicuously, HP1 staining was still relatively homogenously distributed throughout the nucleoplasm (Figure 2E).

For determining whether *kuk* and *kur* have an effect on gene expression, the genome-wide expression profiles in *kuk* and *kur* mutant embryos were compared to those of stage-matched wild-type embryos. We only selected genes with greater than 2-fold change in both genetic conditions. This revealed 96 genes with significant changes in gene expression (Tables S1 and S2). Interestingly, the set of downregulated genes (n = 88) is strongly enriched for early zygotic genes (n = 23), which

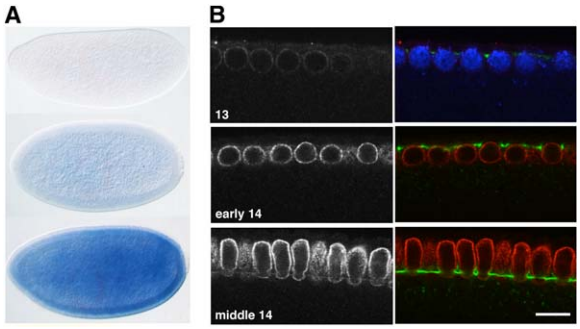

Figure 3. Expression Pattern of *kuk*

(A) In situ hybridization for *kuk* RNA. Embryos prior to pole-cell formation, in cycle 13, and in early cycle 14 (from top).

(B) Wild-type embryos in stages as indicated and stained with Kuk antibody (white, red). The tip of the invaginating membrane is marked by Slam staining (green), and DNA is stained by Dapi (blue, only shown in the upper-right panel). The scale bar represents 10 μm.

are induced during cellularization, e.g., *nullo*, *serendipity*α, *slam*, *bottleneck*, or *frühstart*. In conclusion, in both *kuk* and *kur* embryos, the heterochromatin organization was affected and gene expression was altered. In the following, we will concentrate on the function of *kuk*, because we have not yet revealed the molecular nature of *kur*.

kuk Encodes a Coiled-Coil Protein with Nuclear Localization Signal and CxxM Motif

kuk encodes a protein of 570 amino acid (aa) residues. It contains a putative coiled-coil domain in the N-terminal half of the protein, a nuclear localization signal (NLS), and a C-terminal CxxM-motif, a putative site for farnesylation (Figure S2A). Kuk is so far the first described nuclear protein (see below), except for lamins, that contains a CxxM motif. Comparison with Kuk from other *Drosophila* species revealed an aa identity of 43% between Kuk from *D. melanogaster* and *D. virilis*. By Blast search, we found in the genomes of *Aedes aegyptii* and *Anopheles gambiae* two homologous, not-yet-annotated sequences (Figure S2B), which contained a conserved NLS together with a C-terminal CxxM motif but no obvious coiled-coil region. We did not find any homologous sequences in nonarthropod species.

In wild-type embryos, there is only weak expression of *kuk* during the first 13 division cycles (Figure 3A). In early interphase of cycle 14, *kuk* expression increased significantly. However, in pole cells, *kuk* expression remained constantly low during cellularization. Thus, increase of *kuk* transcription coincides with nuclear elongation.

Localization of Kuk Protein in Embryos

On a cellular level, Kuk appears to be exclusively localized to the nuclear envelope (Figure 3B). The electron-microscope analysis confirmed the nuclear-envelope localization and clearly showed that Kuk exclusively localizes to the nucleoplasmatic side (Figures 4A–4C). As observed by confocal microscopy, Kuk staining only partially overlapped with nuclear pores visualized by antibodies against the nuclear-pore marker Nup50 (Figure 4D). The electron-microscope analysis, however, revealed that Kuk staining is not present at nuclear pores (Figures 4A and 4C).

The antibody staining is specific because RNAi-injected embryos, embryos from *kuk* females (data not shown), and cultured *Drosophila* cells treated with *kuk* dsRNA (see below) lose the nuclear envelope staining for Kuk. Furthermore, the antibody detects recombinant Kuk protein expressed in reticulocyte lysate and *E. coli* as well as endogenous Kuk in extracts from wild-type embryos but not *kuk*-deficient embryos in western blots (Figure S1C).

The immunohistological localization of Kuk was confirmed by biochemical fractionation of embryos. Kuk and Dm0, the *Drosophila* lamin B, were both highly enriched in the nuclear fraction together other nuclear proteins (Figure 5A). Kuk and Dm0 were both not extracted with high-salt but with high-pH buffer (carbonate), consistent with a membrane anchorage by a farnesyl residue. However, Dm0 required higher salt concentration than Kuk for extraction in the presence of 1% triton, suggesting that Kuk in this respect behaves differently than Dm0 and is not part of salt-stable complexes.

The increase of Kuk protein levels during cellularization is comparable to the increase of the mRNA expression levels. In early division cycles 10–13, Kuk staining was very weak (Figure 3E). It strongly increased in early interphase of cycle 14, when cellularization started (Figure 3E). Throughout cellularization, all somatic nuclei showed prominent Kuk staining. The pole cells showed a staining pattern distinct from that of somatic cells. During cycles 10–14, Kuk labeling was absent from the majority of the pole cells (Figure S3A). During mitosis, *kuk* localizes differently than Dm0 or the nuclear-pore marker antibody A141 (Figure S3B). The presence of Kuk in growing late-telophase or interphase nuclei may suggest a function in nuclear-membrane growth.

The localization of some [16] but not all [17] lamina proteins depends on Dm0. In *Dm0*-RNAi-treated cells, the localization of Kuk in the nuclear envelope was indistinguishable from that in control cells (Figures 5B and 5C). However, the localization of Otefin, a Dm0 interacting protein of the INM [18], was changed after *Dm0*-RNAi treatment, confirming the depletion of Dm0. No alterations in the Dm0 localization were observed in *kuk*-RNAi-treated cells. We conclude that Kuk targeting to the nucleoplasmic side of the nuclear envelope and its retention in this subcompartment is independent of Dm0.

Kuk Overexpression in Embryos Results in Highly Lobulated Nuclei

To study the activity of *kuk* in embryos, we injected *kuk* mRNA and fixed the embryos in blastoderm stage. The nuclei became strongly lobulated and wrinkled already early in cellularization (Figure 6B), whereas uninjected embryos possessed smooth, unruffled nuclear envelopes (Figure 6A). Similarily, embryos from transgenic flies with six copies of the *kuk* gene showed very ruffled and abnormally shaped nuclei (Figure 6F). Thus, overexpression of *kuk* resulted in a changed morphology that may be a consequence of extensive growth of the nuclear envelope. In later stages, during gastrulation, moderately wrinkled and lobulated nuclear shapes are typical for interphase nuclei (Figure 6D). In contrast, nuclei

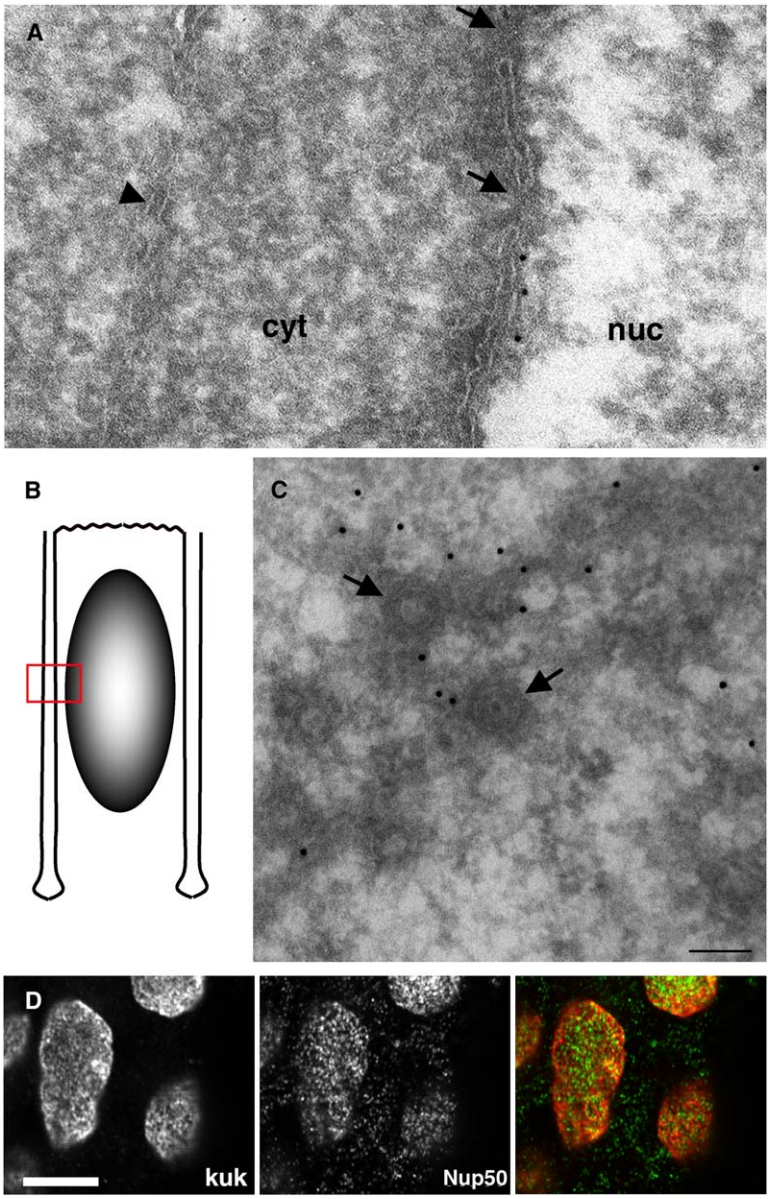

Figure 4. Localization of Kuk

(A) Immunoelectron microscopic analysis of embryonic nuclei reveals localization of Kuk at the inner nuclear membrane (black dots, 10 nm gold particles); arrows indicate nuclear pores, and arrowheads indicate cytoplasmic membranes; cyt denotes cytoplasm, and nuc denotes nucleoplasm.

(B) Schematic drawing of nucleus and invaginating membrane. Red rectangle indicates position of section shown in (A).

(C) Immunolabeling with Kuk antibodies in a tangential section of a nucleus (10 nm gold particles). Several nuclear pores (arrows) are visible (scale bar represents 100 nm). Kuk does not localize to nuclear pores.

(D) Amnioserosa nuclei from late embryos double-labeled with Kuk (red) and Nup50 (green) antibodies. The scale bar represents 5 μm.

in *kuk*-RNAi-treated embryos or embryos from *kuk* females were round and unruffled (Figure 6E). In conclusion, we observed a correlation of the expression of *kuk* and ruffled nuclear morphology.

To test whether *kur* functions independently of *kuk*, we injected *kuk* dsRNA into *kur* embryos. However, there was no visible alteration from the *kuk* phenotype in those RNAi-treated embryos. When we overexpressed *kuk* mRNA in *kur* embryos, a comparable phenotype to overexpression in wild-type embryos was observed (Figure 6C). This indicates that *kur* may function either upstream or independently of *kuk*.

kuk Affects Nuclear Morphology in *Xenopus* Cells

Kuk localizes exclusively to the nuclear envelope when expressed in *Xenopus* A6 cells (Figures 6G–6J). The transfected nuclei became significantly larger (nuclear perimenter is almost doubled, $p < 0.001$, Figure 7G), and the nuclear envelope was more folded, containing deep indentations, compared to nuclei of untransfected control cells (Figures 6G–6J). Costaining for Kuk and XLam B2 revealed strict colocalization of Kuk with lamin B2 over the entire nuclear envelope, including additional intranuclear structures (Figures 6G and 6H). The costaining with Concanavalin A indicates that these intranuclear structures contain membranes and may represent deep indentations of the nuclear envelope (Figures 6I and 6J; [19–21]).

A drastic nuclear-surface enlargement accompanied by the presence of membranous structures inside the nucleus (Figure 6K) was observed by transmission electron microscopy. These additional structures within the nucleus (Figure 6L, asterisks) consisted of double membranes that enclose membrane profiles and ribosomes, structures typical for the cytoplasmic compartment. There were no obvious nuclear pores visible in these intranuclear membranes. Conclusively, the ectopic expression of *kuk* in A6 cells caused primarily nuclear

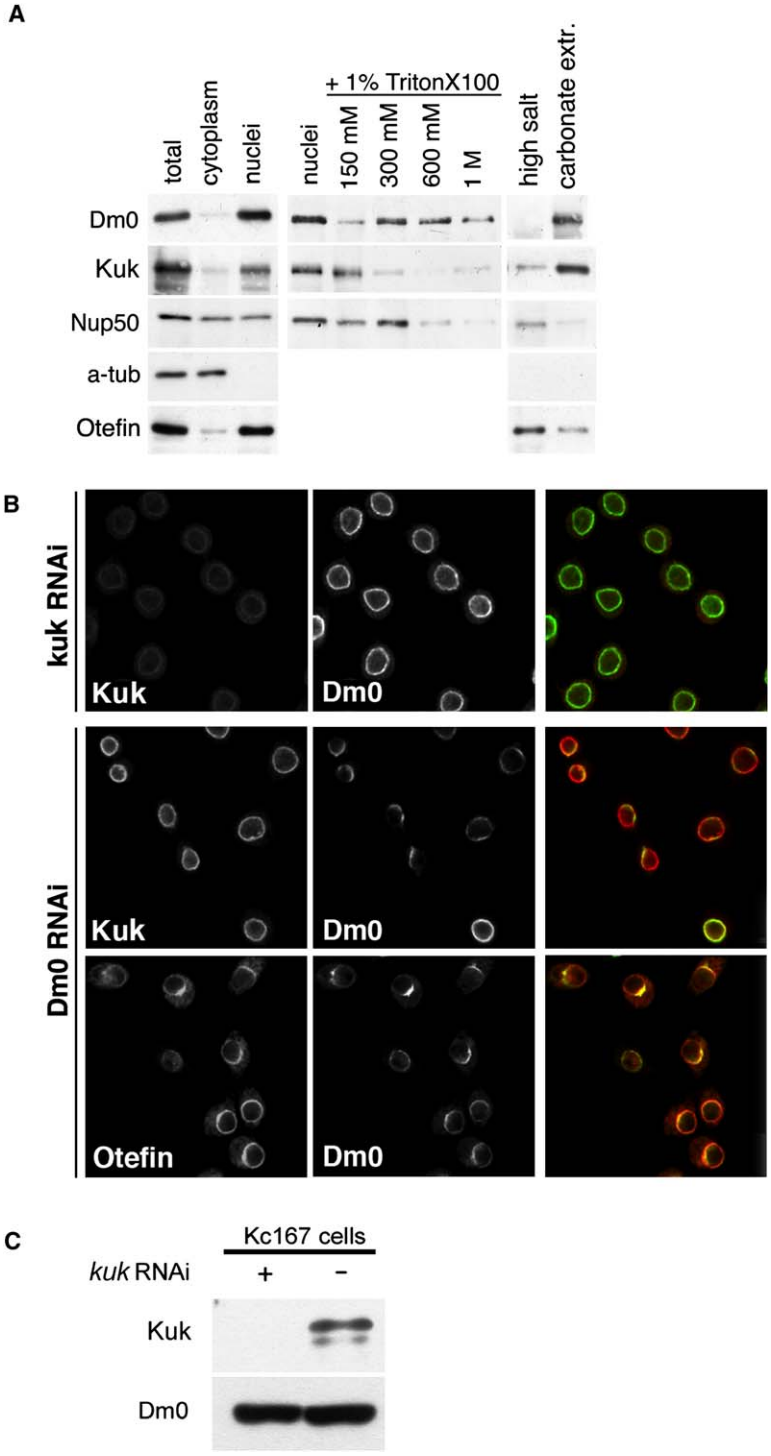

Figure 5. Kugelkern and LaminDm0 Have Independent Functions

(A) Subcellular fractionation and sequential extraction with increasing concentrations of NaCl (α-tub, α- tubulin).

(B) Downregulation of *kuk* and *Dm0*. *Drosophila* Kc167 cells treated with *kuk* or *Dm0* dsRNA were stained for Kuk (white, red), Dm0 (white, green), and Otefin (white, red) as indicated.

(C) Extracts of Kc167 cells treated with *kuk* dsRNA analyzed by western blot with indicated antibodies.

growth that manifests in an extended nuclear surface together with an altered morphology of the nucleus. The activity of *kuk* in *Xenopus* cells suggests that *kuk* employs a conserved mechanism to control nuclear morphology.

All Three Motifs Are Required for Kuk Activity

To characterize the function of the three different structural components of Kuk in detail, we expressed a series of truncated proteins and a nonfarnesylatable mutant version of Kuk (KukSxxM, Figure 7F). Kuk-SxxM and the deletion protein C489 were distributed evenly throughout the nucleoplasm and did not affect nuclear size and shape (Figure 7A). Deletion proteins missing the NLS were homogenously localized in the cell (Figure 7C, mutant C328). Deletion proteins lacking N-terminal aa residues (N136, N275) were located at the nuclear envelope. However, alterations in nuclear morphology were only present in cells expressing a mutant that contained the coiled-coil region (N136, Figures 7D and 7G).

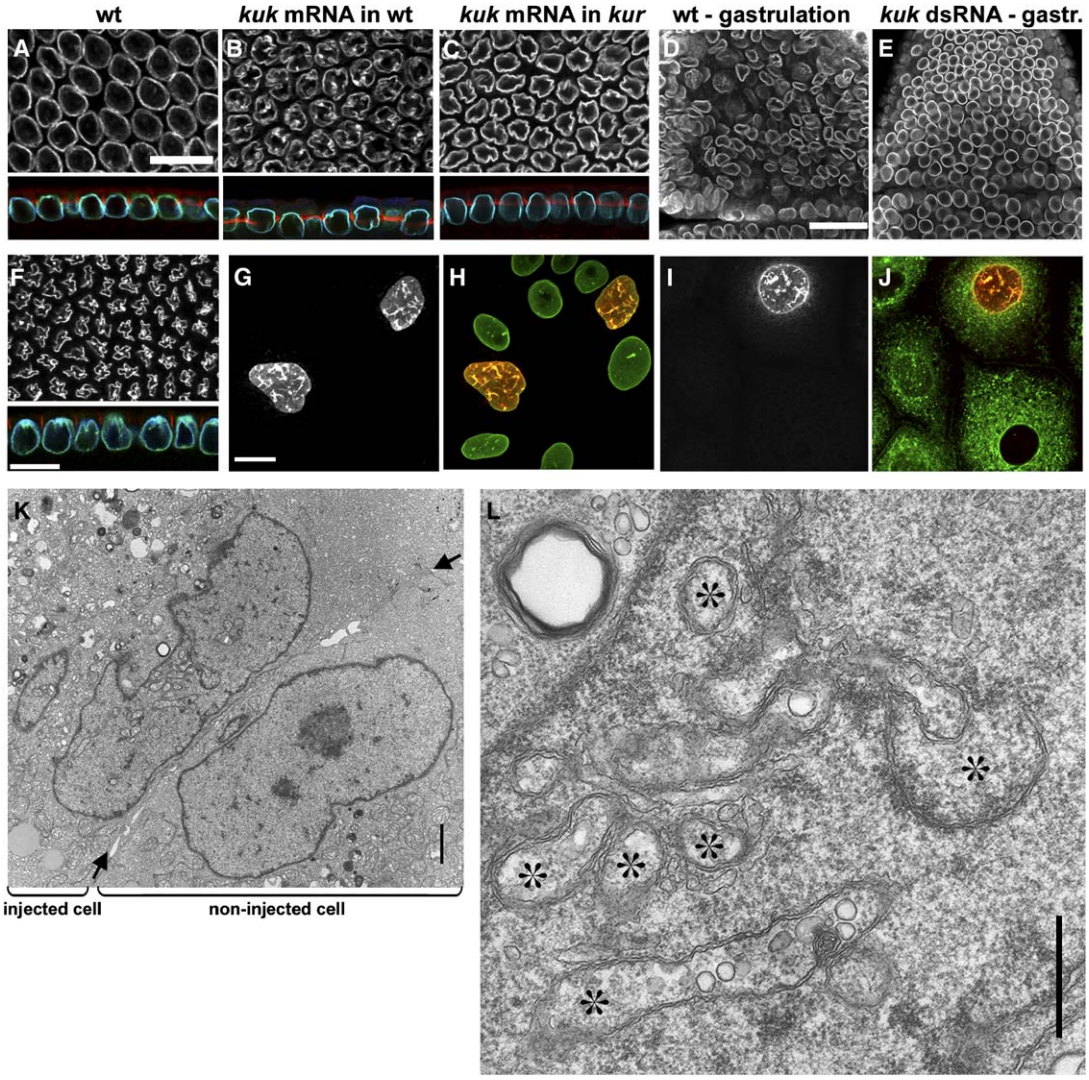

Figure 6. *kugelkern* Induces Nuclear-Membrane Growth

(A–C) Tangential (upper panels) and longitudinal (lower panels) section of embryos ([A], wild-type; [B], wild-type injected with *kuk* mRNA; [C], *kur* embryos injected with *kuk* mRNA) early in cellularization, stained for Kuk (white, green), Dm0 (blue), and f-actin (red).

(D and E) Anterior region of a wild-type and *kuk*-RNAi-treated embryo during gastrulation, stained with Dm0. The scale bar (D and E) represents 25 μm.

(F) Embryo with six copies of *kuk* early in cellularization, stained for Kuk (white, green), Dm0 (blue), and Dlg (red).

(G–J) Kuk expression in *Xenopus* A6 cells. Cells transfected with full-length *kuk* construct were stained for Kuk (white, red), XLam B2 ([G], green), and membranes (ConcanavalinA, [J], green). The scale bar represents 10 μm.

(K and L) Intranuclear structures analyzed by transmission electon microscopy. (K) Ultrathin section of a *kuk*-injected and an uninjected control cell. The cell borders are indicated by arrows. The scale bar represents 1 μm. (L) Higher magnification of the *kuk*-expressing nucleus in (G). The lumina of the tubular structures (asterisk) contain vesicles and ribosomes. The scale bar represents 0.5 μm.

Other C-terminal (C153) or N-terminal (N437) deletion mutants lacking most of the molecule were localized in the nucleoplasm as well as the cytoplasm and did not influence the nuclear morphology (Figure 7F). Thus, all three motifs together are required for the morphogenetic activity of Kuk.

Discussion

The morphology of the nuclei changes dramatically during cellularization. We confirmed [14] that nuclear size indeed increases independently of MT. Thus, nuclear shape change and nuclear growth may be two separate processes, regulated independently. We favor the model that nuclear size increase is a nuclear-autonomous process and the growing nuclei are directed passively by the MT basket into an ellipsoidal shape.

What may be the function of Kuk during cellularization? Although the nuclear size increase is impaired in *kuk*- and *kur*-depleted embryos, no other defects, e.g., concerning plasma-membrane invagination or the actin cytoskeleton, are observed. Consistent with the hypothesis that in *kuk* embryos a nuclear-intrinsic process is affected, we find that Kuk exclusively localizes to the INM. Because *kuk* and *kur* embryos show divergent phenotypes during gastrulation, we deduce that *kur* has during

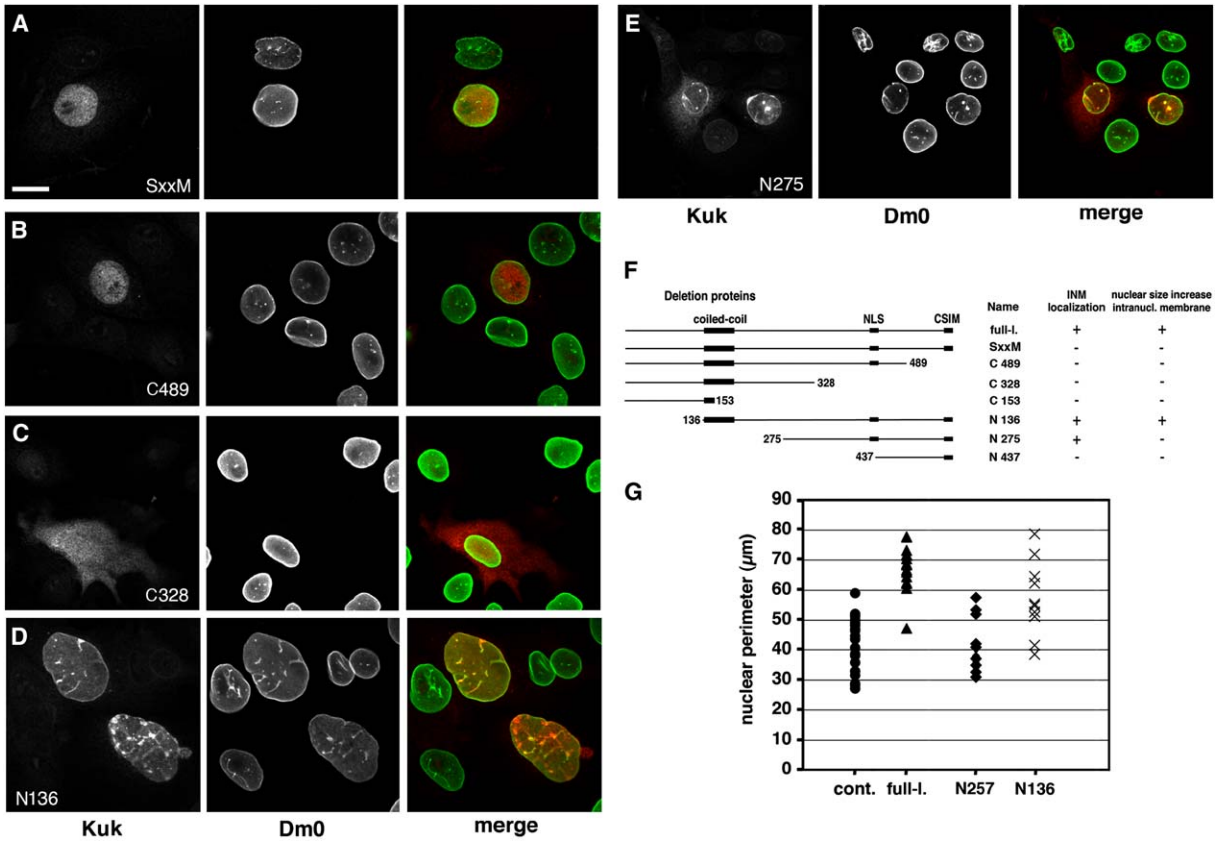

Figure 7. Deletion Mutants of *kuk* Expressed in *Xenopus* A6 Cells

(A–E) *Xenopus* A6 cells transfected with indicated *kuk* constructs and stained for Kuk (white, red) and XLam B2 (white, green).

(F) Schematic overview of the deletion constructs and summary of their activity. NLS denotes nuclear localization signal, and CSIM denotes farnesylation motif. (+) indicates localization of the expressed *kuk* construct to the nuclear envelope (INM) or whether larger nuclei with intranuclear structures were induced.

(G) Quantification of nuclear size by measuring the nuclear perimenter. Bidirectional Mann-Whitney test was applied to *kuk* full-length versus control cells (*kuk*: n = 16, control: n = 30; $p < 0.001$, $U_A = 14$, $z = 5.2$), N136 versus control cells (n = 10, $p = 0.0005$, $U_A = 212$, $z = -3.46$), and N275 versus control cells (n = 16, $p = 0.992$, $U_A = 191$, $z = 0.01$).

development a second, unknown function unrelated to the nuclear-elongation phenotype during cellularization. Insight into the function of *kur* has to await its molecular characterization.

Kuk shares some structural features, such as the nuclear localization signal (NLS), a coiled-coil domain, and the C-terminal CxxM-motif, with B type lamins. Interestingly, up to now, lamins were the only known nuclear proteins possessing a farnesyl moiety [22]. In addition to these similarities, Kuk exhibits properties distinct from that of lamins.

The overexpression of Kuk in embryos results in a nuclear morphology comparable to that found in gastrulating wild-type embryos. In contrast, *kuk*-depleted gastrulating embryos have smooth and unwrinkled nuclei typical for earlier stages. Thus, the overexpression phenotype of *kuk* may reflect precocious growth of the nuclear envelope. In *Xenopus* cells, Kuk induces additional membrane growth, the nuclei become larger, and the nuclear envelope is highly lobulated. By analyzing deletion constructs and a nonfarnesylated mutant of Kuk, we demonstrated that all three motifs, the coiled-coil region, the NLS, and the CxxM motif together are required for the morphogenetic activity of Kuk. These findings are consistent with data from lamin-overexpression experiments in cultured mammalian, amphibian, or fish cells. In these studies, all lamin variants that contain an NLS together with the farnesylation motif show conspicuous overproliferation of NM [19, 22].

It seems unlikely that *kuk* takes part in the general phospholipid synthesis or membrane transport machinery, because in *kuk* embryos we see normal plasma-membrane invagination during cellularization. Most likely, *kuk* is part of a mechanism specific for nuclei. In principle, two different mechanisms are conceivable: (1), a catalytic function, where Kuk might induce membrane growth indirectly by activating effector components; and (2), a structural function, where Kuk might have a direct effect on the structure of the phospholipid bilayer. Insertion of farnesylated Kuk or Lamin B, acting like a wedge, would lead to a modification of the inner phospholipid layer by increasing the lateral packing stress of the membrane. This deformation in turn could induce incorporation of new phospholipids and thus allow expansion of the nuclear-membrane surface area. Consistent with this second model is our estimation of the number of Kuk molecules per nucleus (>10^4/nucleus, compared to >10^5/nucleus of Dm0). A structural model

is supported by studies of the activity of amphiphathic proteins on nuclear morphology. Incorporation of ampiphysin [23], CTP:phosphocholine cytidylyl-transferase-α (CCTα, [20]), or Nup53 [24] into the nuclear envelope induces intranuclear, tubular membranes. Moreover, CCTα and ampiphysin have been shown to affect membrane curvature in vitro [20, 23]. How increased positive membrane curvature of the INM leads to the growth of the entire nuclear envelope remains to be elucidated.

Coincidental with nuclear elongation is the onset of zygotic transcription together with the rearrangement of the chromatin architecture. Strikingly, in both *kuk* and *kur* embryos, the reorganization of the chromatin is affected. Because this difference in chromatin organization is found independently in *kuk* as well as in *kur* embryos, we conclude that this phenotype might be related to the reduced nuclear size or nuclear surface area in both mutants. HP1 is known to be associated with heterochromatin and to influence gene expression [13, 25]. It can also interact with the inner nuclear-membrane protein LBR (Lamin B receptor, [26]) and thus may represent an adaptor between nuclear lamina and chromatin [27]. Indeed, we found that gene expression is altered in *kuk* and *kur* embryos. Convincingly, a specific set of genes are downregulated in both *kuk* and *kur* embryos in parallel, which suggests a connection between reduced nuclear surface area and transcriptional regulation. It is clear, however, that the nuclear elongation is not essential but only contributes to full onset of gene expression during cellularization.

Mutations in proteins of the lamina cause a wide range of human diseases, collectively called laminopathies [5], e.g., Hutchinson-Gilford progeria syndrome (HGPS), where a dominant point mutation in the *LMNA* gene causes a premature-accelerated-aging-like disorder [28, 29]. In the HGPS cells, the *LMNA* precursor is not properly endoproteolytically processed, resulting in a mutated lamin A form that still contains a farnesylated C terminus. Cultured fibroblasts from HGPS patients show pronounced lobular nuclear shapes that correlate with defects in DNA replication and alteration in heterochromatin organization [5, 27]. Moreover, lymphocytes directly isolated from HGPS patients possess strikingly enlarged nuclei [28]. Cells depleted for the endoprotease FACE1/Zmpste24, the enzyme that cleaves the farnesylated C terminus of the premature lamin A, show similar dramatic changes in the nuclear morphology with extensively lobulated nuclei [9]. These similarities between the phenotypes of HGPS cells and cells overexpressing nuclear proteins, such as Kuk, B type lamins, or uncleaved lamin A, with a farnesylation motif might have implications for our understanding of the Hutchinson-Gilford progeria syndrome.

Conclusions

The nuclear lamina controls the shape of the nucleus but also interacts with chromatin to regulate gene expression. Analyzing the control of nuclear shape in a simple genetic system will allow better investigation of the function of the lamina and its connection to the control of gene expression. One can speculate that overexpression of Kuk or Dm0 in adult flies may cause aging-like symptoms or even influences life span. The finding that the structural motifs coiled-coil, NLS, and CxxM are characteristic for lamins as well as for nonlamins like Kuk can help to screen for more, functionally important nuclear envelope proteins.

Experimental Procedures

General Procedures

A comprehensive and detailed description of the methods and materials can be found in the Supplemental Data.

kuk (CG5175) was identified in a project that was initiated to reveal the function of early zygotic genes and was performed in a collaboration of the laboratories of T.L and J.G. [30]. fs(1)*kur* maps to 2B17;3C6 and was isolated in a screen for blastoderm mutants (A.B., F.P, and J. G., unpublished data) from a collection of germline clone mutations (N.V., unpublished data) similar to the collection described by S. Luschnig [31]. Embryological procedures were applied according to standard protocols [32]. The microarray data were deposited to EBI MIAMExpress; see Accession Numbers.

Histology

Embryos and *Xenopus* A6 and *Drosophila* Kc167 cells were fixed and stained according to standard procedures (Supplemental Data, [19, 33]). In some cases, 0.5% Triton X-100 was added to the blocking solution to improve permeabilization.

Drug Treatment

For nocodazole treatment, dechorionated embryos were incubated for 2.5 min in n-heptane to permeabilize the vitelline membrane, briefly rinsed in PBS + 0.1% Tween, incubated for 50 min at room temperature in PBS containing 50 μg/ml nocodazole, and subsequently fixed with FA.

Transfection and Microinjection of Cells

Cells were fixed and stained 24–48 hr after transfection. Microinjection together with a GFP construct and EM processing was performed according to [19, 33].

Microscopy

Control embryos were always mounted on the same slide and processed in parallel. For comparing the relative fluorescence levels of HP1 staining along the apical-basal axis of the nuclei, 10 nuclei in each 5 *kur*- and *kuk*-RNAi-treated embryos were evaluated.

Supplemental Data

Supplemental Data include Supplemental Experimental Procedures, three figures, and two tables and are available with this article online at: http://www.current-biology.com/cgi/content/full/16/6/543/DC1/.

Acknowledgments

We thank D. Görlich, K. Kapp, F. Schnorrer, M. Seedorf, and the lab members for discussions, advice, and suggestions on the manuscript. We thank Y. Kussler-Schneider for technical assistance; K. Schild for microinjection and processing for EM; S. Panier, S. Lawo, and P. Gawlinski for antibody purification and characterization and initial fractionation experiments; S. Lawo for western in Figure S3B; and D.T. and A.M. Brandt for support. We are grateful for materials, reagents, and fly stocks from D. Görlich, M. Hild, Drosophila Stock Center (Bloomington, Indiana), and Hybridoma bank (Iowa). N.V. was supported by the Boehringer Ingelheim Fonds, A.B. by a Forschungsstipendium of the Deutsche Forschungsgemeinschaft, and J.G. by the Emmy-Noether Programm of the Deutsche Forschungsgemeinschaft.

Received: December 20, 2005
Revised: January 21, 2006
Accepted: January 24, 2006
Published online: February 2, 2006

References

1. Haithcock, E., Dayani, Y., Neufeld, E., Zahand, A.J., Feinstein, N., Mattout, A., Gruenbaum, Y., and Liu, J. (2005). Age-related changes of nuclear architecture in *Caenorhabditis elegans*. Proc. Natl. Acad. Sci. USA *102*, 16690–16695.
2. Goldman, R.D., Shumaker, D.K., Erdos, M.R., Eriksson, M., Goldman, A.E., Gordon, L.B., Gruenbaum, Y., Khuon, S., Mendez, M., Varga, R., et al. (2004). Accumulation of mutant lamin A causes progressive changes in nuclear architecture in Hutchinson-Gilford progeria syndrome. Proc. Natl. Acad. Sci. USA *101*, 8963–8968.
3. Gisselsson, D., Bjork, J., Hoglund, M., Mertens, F., Dal Cin, P., Akerman, M., and Mandahl, N. (2001). Abnormal nuclear shape in solid tumors reflects mitotic instability. Am. J. Pathol. *158*, 199–206.
4. Gruenbaum, Y., Goldman, R.D., Meyuhas, R., Mills, E., Margalit, A., Fridkin, A., Dayani, Y., Prokocimer, M., and Enosh, A. (2003). The nuclear lamina and its functions in the nucleus. Int. Rev. Cytol. *226*, 1–62.
5. Gruenbaum, Y., Margalit, A., Goldman, R.D., Shumaker, D.K., and Wilson, K.L. (2005). The nuclear lamina comes of age. Nat. Rev. Mol. Cell Biol. *6*, 21–31.
6. Lenz-Böhme, B., Wismar, J., Fuchs, S., Reifegerste, R., Buchner, E., Betz, H., and Schmitt, B. (1997). Insertional mutation of the *Drosophila* nuclear lamin Dm0 gene results in defective nuclear envelopes, clustering of nuclear pore complexes, and accumulation of annulate lamellae. J. Cell Biol. *137*, 1001–1016.
7. Cohen, M., Lee, K.K., Wilson, K.L., and Gruenbaum, Y. (2001). Transcriptional repression, apoptosis, human disease and the functional evolution of the nuclear lamina. Trends Biochem. Sci. *26*, 41–47.
8. Krohne, G. (1998). Lamin assembly in vivo. Subcell. Biochem. *1*, 563–586.
9. Varela, I., Cadinanos, J., Pendas, A.M., Gutierrez-Fernandez, A., Folgueras, A.R., Sanchez, L.M., Zhou, Z., Rodriguez, F.J., Stewart, C.L., Vega, J.A., et al. (2005). Accelerated ageing in mice deficient in Zmpste24 protease is linked to p53 signalling activation. Nature *437*, 564–568.
10. Foe, V.E., Odell, G., and Edgar, B. (1993). Mitosis and morphogenesis in the *Drosophila* embryo: point and counterpoint. In The Development of *Drosophila melanogaster*, M. Bate and A. Martinez Arias, eds. (New York: Cold Spring Harbor Laboratory Press), pp. 149–300.
11. Schejter, E.D., and Wieschaus, E. (1993). Functional elements of the cytoskeleton in the early *Drosophila* embryo. Annu. Rev. Cell Biol. *9*, 67–99.
12. Sonnenblick, B.P. (1950). The early embryology of *Drosophila melanogaster*. In Biology of *Drosophila*. M. Demerec, ed. (New York: Wiley and Son), pp. 62–167.
13. Kellum, R., Raff, J.W., and Alberts, B.M. (1995). Heterochromatin protein 1 distribution during development and during the cell cycle in *Drosophila* embryos. J. Cell Sci. *108*, 1407–1418.
14. Edgar, B.A., Odell, G.M., and Schubiger, G. (1987). Cytoarchitecture and the patterning of fushi tarazu expression in the *Drosophila* blastoderm. Genes Dev. *1*, 1226–1237.
15. Irvine, K.D., and Wieschaus, E. (1994). Cell intercalation during *Drosophila* germband extension and its regulation by pair-rule segmentation genes. Development *120*, 827–841.
16. Wagner, N., Schmitt, J., and Krohne, G. (2004a). Two novel LEM-domain proteins are splice products of the annotated *Drosophila melanogaster* gene CG9424 (Bocksbeutel). Eur. J. Cell Biol. *82*, 605–616.
17. Wagner, N., Weber, D., Seitz, S., and Krohne, G. (2004b). The lamin B receptor of *Drosophila melanogaster*. J. Cell Sci. *117*, 2015–2028.
18. Goldberg, M., Lu, H., Stuurman, N., Ashery-Padan, R., Weiss, A.M., Yu, J., Bhattacharyya, D., Fisher, P.A., Gruenbaum, Y., and Wolfner, M.F. (1998). Interactions among *Drosophila* nuclear envelope proteins lamin, otefin, and YA. Mol. Cell. Biol. *18*, 4315–4323.
19. Prüfert, K., Vogel, A., and Krohne, G. (2004). The lamin CxxM motif promotes nuclear membrane growth. J. Cell Sci. *117*, 6105–6116.
20. Lagace, T.A., and Ridgway, N.D. (2005). The rate-limiting enzyme in phosphatidylcholine synthesis regulates proliferation of the nucleoplasmic reticulum. Mol. Biol. Cell *16*, 1120–1130.
21. Fricker, M., Hollinshead, M., White, N., and Vaux, D. (1997). Interphase nuclei of many mammalian cell types contain deep, dynamic, tubular membrane-bound invaginations of the nuclear envelope. J. Cell Biol. *136*, 531–544.
22. Ralle, T., Grund, C., Franke, W.W., and Stick, R. (2004). Intranuclear membrane structure formations by CaaX-containing nuclear proteins. J. Cell Sci. *117*, 6095–6104.
23. Peter, B.J., Kent, H.M., Mills, I.G., Vallis, Y., Butler, P.J., Evans, P.R., and McMahon, H.T. (2004). BAR domains as sensors of membrane curvature: the amphiphysin BAR structure. Science *303*, 495–499.
24. Marelli, M., Lusk, C.P., Chan, H., Aitchison, J.D., and Wozniak, R.W. (2001). A link between the synthesis of nucleoporins and the biogenesis of the nuclear envelope. J. Cell Biol. *153*, 709–724.
25. Piacentini, L., Fanti, L., Berloco, M., Perrini, B., and Pimpinelli, S.J. (2003). Heterochromatin protein 1 (HP1) is associated with induced gene expression in *Drosophila* euchromatin. J. Cell Biol. *161*, 671–672.
26. Ye, Q., Callebaut, I., Pezhman, A., Courvalin, J.C., and Worman, H.J. (1997). Domain-specific interactions of human HP1-type chromodomain proteins and inner nuclear membrane protein LBR. J. Biol. Chem. *272*, 14983–14989.
27. Scaffidi, P., and Misteli, T. (2005). Reversal of the cellular phenotype in the premature aging disease Hutchinson-Gilford progeria syndrome. Nat. Med. *11*, 440–445.
28. De Sandre-Giovannoli, A., Bernard, R., Cau, P., Navarro, C., Amiel, J., Boccaccio, I., Lyonnet, S., Stewart, C.L., Munnich, A., Le Merrer, M., et al. (2003). Lamin a truncation in Hutchinson-Gilford progeria. Science *300*, 2055.
29. Eriksson, M., Brown, W.T., Gordon, L.B., Glynn, M.W., Singer, J., Scott, L., Erdos, M.R., Robbins, C.M., Moses, T.Y., Berglund, P., et al. (2003). Recurrent de novo point mutations in lamin A cause Hutchinson-Gilford progeria syndrome. Nature *423*, 293–298.
30. Pilot, F., Philippe, J.M., Lemmers, C., Chauvin, J.P., and Lecuit, T. (2006). Developmental control of nucler morphogenesis and anchoring by charleston, identified in a functional genomic screen of *Drosophila* cellularisation. Development *133*, 711–723.
31. Luschnig, S., Moussian, B., Krauss, J., Desjeux, I., Perkovic, J., and Nusslein-Volhard, C. (2004). An F1 genetic screen for maternal-effect mutations affecting embryonic pattern formation in *Drosophila melanogaster*. Genetics *167*, 325–342.
32. Roberts, D.B. (1998). *Drosophila*, A Practical Approach. (Oxford, UK: Oxford University Press).
33. Prüfert, K., Alsheimer, M., Benavente, R., and Krohne, G. (2005). The myristoylation site of meiotic lamin C2 promotes local nuclear membrane growth and the formation of intranuclear membranes in somatic cultured cells. Eur. J. Cell Biol. *84*, 637–646.

Accession Numbers

The microarray data were deposited to EBI MIAMExpress with the accession numbers E-TABM-75 (data) and A-MEXP-314 (array design).